

Eigenvalue Signal Processing for Weather Radar Polarimetry: Removing the Bias Induced by Antenna Coherent Cross-Channel Coupling

Michele Galletti, Dusan S. Zrnica, *Fellow, IEEE*, Frank Gekat, and Peter Goelz

Abstract—We present a novel digital signal processing procedure, named eigenvalue signal processing (henceforth ESP), patented by the first author with Brookhaven Science Associates in 2013. The method enables the removal of the bias due to antenna coherent cross-channel coupling and is applicable in the LDR mode, the ATSR mode and the STSR orthogonal mode of weather radar measurements. In this paper, we focus on the LDR mode and consider copolar reflectivity at horizontal transmit (Z_{HH}), cross-polar reflectivity at horizontal transmit (Z_{VH}), linear depolarization ratio at horizontal transmit (LDR_H) and degree of polarization at horizontal transmit (DOP_H). The ESP (ESP) method is substantiated by an experiment carried out in November 2012 using C-band weather radar with a parabolic reflector located at the Selex ES—Gematronik facilities in Neuss, Germany. The experiment involved comparison of weather radar measurements taken 1.5 minutes apart in two hardware configurations, namely with cross-coupling on (cc-on) and cross-coupling off (cc-off). It is experimentally demonstrated that eigenvalue-derived variables are invariant with respect to antenna coherent cross-channel coupling. This property had to be expected, since the eigenvalues of the Coherency matrix are SU(2) invariant.

Index Terms—Antenna radiation pattern, coherency matrix, copolar radiation pattern, covariance matrix, cross-channel coupling, cross-polar correlation coefficient, cross-polar radiation pattern, degree of polarization at horizontal transmit, eigenvalues, linear depolarization ratio, polarimetric phased array weather radar.

I. INTRODUCTION

THE development of polarimetric phased array weather radars is critical for the Multi-function Phased Array Radar (MPAR) mission. The major technological challenge in phased array weather radar polarimetry is attaining an acceptable cross-polar isolation between the H and V channels of the radar system. The present paper proposes Eigenvalue Signal Processing (ESP) to mitigate the problem of antenna cross-polarization isolation, and is potentially suitable for implementation in polarimetric phased array antennas, but also in conventional parabolic reflectors. A prerequisite for the under-

standing of the present paper is [1]. The Degree of Polarization at Horizontal/Vertical transmit is the theoretical centerpiece that permits the derivation of unbiased estimates of Reflectivity Z , Linear Depolarization Ratio LDR, and Differential Reflectivity Z_{DR} . The strength of the ESP approach resides in the fact that bias correction is obtained without knowing the actual amount of antenna cross-polar coupling. Indeed, the cross-polar correlation coefficients at horizontal and vertical transmit (ρ_{xh} and ρ_{xv}) do provide an intrinsic measurement of antenna coherent cross-channel coupling [1, eq. (66)], and the diagonalization of the Coherency matrices at horizontal and vertical polarizations automatically removes the bias from the two diagonal elements. This aspect is crucial: in the framework herein described, bias correction does not involve multiplying the retrieved scattering matrix with a “correction” matrix. The latter requires calibration to be performed on a beam-by-beam basis and, especially for large phased-arrays, it would render the engineering task daunting. Eigenvalue Signal Processing cannot retrieve unbiased scattering matrices but, under the reasonable assumption of target reflection symmetry [2], it can retrieve the unbiased Coherency matrices at horizontal and vertical polarization transmit, providing unbiased estimates for reflectivity Z , differential reflectivity Z_{DR} , and linear depolarization ratio LDR.

ESP hinges on three theoretical pillars:

- 1) The assumption that weather scatterers possess reflection symmetry [2], that is, they are non-canted and their intrinsic cross-polar correlation coefficients (ρ_{xh} and ρ_{xv}) are equal to 0. We remind the reader that target reflection symmetry also underpins the choice of the STSR hybrid polarimetric architecture in present-day weather radars at S, C, and X bands (e.g., NEXRAD) and is therefore considered to be a safe assumption [3].
- 2) The invariance of Degree of Polarization at Horizontal/Vertical transmit with respect to antenna coherent coupling. An exhaustive analysis of DOP_H is provided in [1]. Together with the previous point, DOP_H invariance allows the derivation of an unbiased estimate for LDR, in the following named LDR_{ESP} .
- 3) The invariance of the trace of the coherency matrix with respect to antenna coherent coupling. This allows the derivation of unbiased estimate for Z , in the following named Z_{ESP} . Application of the same procedure to the two Coherency matrices at H and V transmit yields an unbiased estimate for differential reflectivity Z_{DR} , in the following named Z_{DR_ESP} .

Manuscript received July 29, 2013; revised October 11, 2013, January 14, 2014, and March 7, 2014; accepted April 4, 2014.

M. Galletti is with the Brookhaven National Laboratory, Environmental and Climate Sciences Department, U.S. Department of Energy, Upton, NY 11973 USA (e-mail: mgalletti@bnl.gov).

D. S. Zrnica is with the National Severe Storms Laboratory, National Oceanic and Atmospheric Administration, Norman, OK 73072 USA.

F. Gekat and P. Goelz are with Selex ES GmbH, 41470 Neuss, Germany.

Color versions of one or more of the figures in this paper are available online at <http://ieeexplore.ieee.org>.

Digital Object Identifier 10.1109/TGRS.2014.2316821

From a superior viewpoint, there is only one theoretical principle underlying ESP: SU(2) transformations [4] are an accurate mathematical representation of coherent antenna coupling acting on the antenna height spinor both on transit and receive (a derivation of the contravariant antenna height spinor and of the covariant wave spinor is presented in [4]). ESP theory provides an algebraic proof that the largest and smallest eigenvalues of the Coherency matrix correspond to the copolar and cross-polar powers measured by an antenna that is perfectly aligned with the principal axes of the illuminated distributed scatterer. In fact, Eigenvalue Signal Processing produces an alignment between the illuminated scatterers, (assumed to possess reflection symmetry and therefore characterized by intrinsic cross-polar correlation coefficients ρ_{xh} and ρ_{xv} equal to zero) and the antenna height spinor (assumed to be slightly tilted from the horizontal/vertical because of coherent cross-channel coupling). The alignment is produced by means of the diagonalization of the coherency matrices at horizontal and vertical transmit \mathbf{J}_H and \mathbf{J}_V . The source of the “misalignment” is ascribed to the coherent cross-polar power radiated by the antenna inducing positive non-zero cross-polar correlation coefficients. In a loose analogy, Eigenvalue Signal Processing is for distributed (stochastic) scatterers what the Graves Power matrix theory is for single scatterers [5], [6]. In both cases the eigenvalues correspond to powers in the “aligned” reference frame. Application of ESP is also effective for the removal of bias caused by forward scattering due to propagation through canted scatterers, usually visible as stripes of higher LDR and ρ_{xh} along the radials as shown in [7] for the degree of polarization at horizontal transmit.

Even though the present body of work originated within the synthetic aperture radar (SAR) polarimetry community [8]–[10], it has substantially departed from it, especially because all variables treated in the present paper (ESP variables) are obtained from the eigenvalues of the 2×2 Coherency matrices \mathbf{J}_H and \mathbf{J}_V , whereas in the SAR polarimetry community focus is on eigenvalue- and eigenvector-derived variables of the 3×3 Covariance matrix \mathbf{C} [9]. Operating on the 2×2 Coherency matrices involves SU(2) transformations, whereas operating on the 3×3 Covariance matrix involves SU(3) transformations. This aspect is fundamental and should not be overlooked. SU(2) describes a set of transformations that exactly corresponds to the set of polarization basis transformations, and therefore describes all the possible distortions imposed by the antenna on the radiated polarization state. The eigen-analysis of the Coherency matrices cannot obviously provide information about the 1, 3 term of the 3×3 Covariance matrix, information traditionally encapsulated in the copolar correlation coefficient ρ_{hv} and differential phase Ψ_{DP} . Eigen-analysis of the 3×3 Covariance matrix can however provide eigenvalue- and eigenvector-derived variables—scattering entropy H and the alpha angle α —which are good proxies for ρ_{hv} and differential phase ($\Psi_{DP} = \Phi_{DP} + \delta_{co}$), respectively [11], [12]. In this case however, SU(3) spans a set of transformations that are larger (in the strict sense) than the set of polarization bases transformations [8], and the correspondence between eigen-variables (H , α) and their traditional counterparts (ρ_{hv} and Ψ_{DP}) is only approximate.

In the following, we will only focus on variables derived from the eigenvalues of the Coherency matrices \mathbf{J}_H and \mathbf{J}_V . The ESP variables defined in the following (Z_{ESP} , Z_{DR_ESP} , LDR_{ESP}) are antenna-unbiased replacements for standard radar meteorological variables obtained from the diagonal of the Covariance (Coherency) matrix: Reflectivity Z , Differential Reflectivity Z_{DR} and Linear Depolarization Ratio LDR .

A. Polarimetric Operating Modes and Orthogonal Waveforms

Eigenvalue Signal Processing requires orthogonal polarization bases and is therefore applicable when the radar operates at LDR mode (Linear Depolarization Ratio mode), ATSR mode (Alternate Transmission Simultaneous Receive mode) or STSR orthogonal mode [Simultaneous Transmission Simultaneous Receive orthogonal mode—Fig. 1(b) and (c)], but it is not applicable at STSR hybrid mode [Simultaneous Transmission Simultaneous Receive hybrid mode Fig. 1(a)]. LDR mode corresponds to horizontal polarization transmit, and simultaneous reception of H and V; ATSR mode corresponds to H transmit and simultaneous H and V receive, followed by V transmit and simultaneous H and V receive. STSR hybrid mode [Fig. 1(a)] corresponds to Simultaneous Transmission of H and V and Simultaneous Reception of H and V; here, hybrid indicates that the receive polarization basis is not copolar and cross-polar to the transmit polarization. STSR hybrid mode is the default choice for operational weather radars (see also Table I). STSR orthogonal corresponds to the simultaneous transmission and simultaneous reception of orthogonal H and V waveforms, with the capability of retrieving the four components of the scattering matrix $\mathbf{S}(S_{hh}, S_{hv}, S_{vh}, S_{vv})$ in one pulse repetition time, instead of two as in the ATSR mode [13]–[15]. In this case, the word orthogonal refers to the two waveforms used to simultaneously excite the H and V channels, but may also refer to the fact that, using waveform diversity, the polarization basis in use is orthogonal even though the two pulses are radiated simultaneously. ESP is fully compatible with the use of waveform diversity in the radar system, since ESP relies on processing performed on the elements of the 2×2 Coherency matrices, that involve correlations of each of the two waveforms with itself, but do not involve correlations between the two different waveforms (the latter appearing only in the 1,3 and 3,1 terms of the 3×3 Covariance matrix). In Fig. 1(b) and (c) we consider two orthogonal waveforms, where the term orthogonal refers to their disjoint spectral support. Other definitions of orthogonal waveforms exist, for example phase-coded waveforms may be termed orthogonal even if their spectral support is overlapping. In any case, ESP is always compatible with waveform diversity, either spectrally disjoint, or phase-coded waveforms, provided the 2×2 Coherency matrix is measured. STSR orthogonal modes are looked at with increasing interest for phased array weather radar polarimetry, due to its property of lowering the isolation requirement on cross-polar isolation to the levels of the ATSR mode (requirement for ATSR and STSR orthogonal modes is -25 dB, whereas for STSR hybrid it is around -45 dB [16]).

Besides lowering the requirement for antenna isolation to the levels of the ATSR mode, the use of orthogonal waveforms also

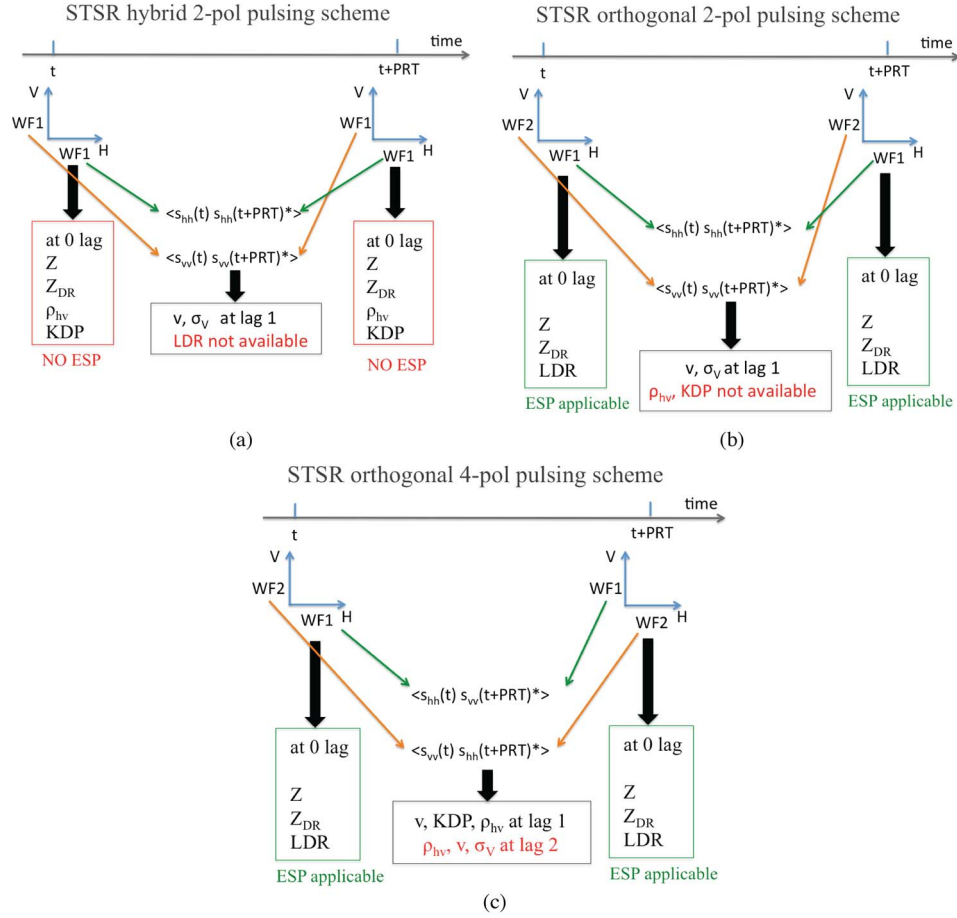


Fig. 1. (a) STSR hybrid 2-pol mode. The same waveform (WF1) excites simultaneously the H and V channels, yielding estimates of Z , Z_{DR} , ρ_{hv} and KDP at 0 lag. This operating mode is the standard in use for weather radar systems at S, C, and X bands (e.g., NEXRAD). In this operating mode, ESP is not applicable, since transmit and receive polarization states are not orthogonal (hence the term hybrid). Also, LDR is not available in this mode. (b) STSR orthogonal 2-pol mode. Two orthogonal waveforms (WF1 and WF2) are used to excite the H and V channels. This yields 0-lag measurements of Z , Z_{DR} and LDR (for which ESP is applicable), yet prevents the estimation of ρ_{hv} and KDP since the correlation of the two orthogonal waveforms (with disjoint spectral support) is 0. (c) STSR orthogonal 4-pol mode. Two orthogonal waveforms (WF1 and WF2) are used to excite the H and V channels by switching between Waveform 1 (WF1) and Waveform 2 (WF2) on a pulse-to-pulse basis. This operating mode yields Z , Z_{DR} and LDR at 0 lag (for which ESP is applicable) and radial velocity v , copolar correlation coefficient ρ_{hv} and KDP at 1 lag [17], [18] in the same scan time as the STSR hybrid 2-pol pulsing scheme [Fig. 1(a)]. The drawback is that estimation of the copolar correlation coefficient ρ_{hv} at lag 0 requires the estimation of the signal autocorrelation at lag 2 as indicated in the denominator of equation 6.90 in [18].

TABLE I
POLARIMETRIC ARCHITECTURES FOR WEATHER RADARS

<i>Polarimetric Architecture</i>	<i>Standard Variables</i>	<i>ESP variables</i>
LDR mode (2-pol)	Z LDR	Z_{ESP} LDR_{ESP}
STSR hybrid mode (2-pol)	Z Z_{DR} ρ_{hv} KDP	None
ATSR mode (4-pol)	Z LDR Z_{DR} ρ_{hv} KDP	Z_{ESP} LDR_{ESP} Z_{DR_ESP}
STSR orthogonal mode (4-pol)	Z LDR Z_{DR} ρ_{hv} KDP	Z_{ESP} LDR_{ESP} Z_{DR_ESP}

permits the implementation of polarimetry in less scan time than the ATSR mode or, equivalently, in the same scan time as the STSR hybrid mode. As an application example, we consider two orthogonal waveforms WF1 and WF2 with disjoint spectral support such that their correlation is 0. Switching between the two waveforms in the H and V channels as indicated in Fig. 1(c) (STSR orthogonal 4-pol mode) allows one to retrieve all polarimetric variables in the same scan time as the STSR hybrid mode [Fig. 1(a)]. The STSR orthogonal 4-pol mode [Fig. 1(c)] yields Z , Z_{DR} and LDR at 0 lag (for which ESP is applicable), it yields velocity v and KDP at 1 lag [17] and yields

the copolar correlation coefficient ρ_{hv} at 1 lag (equation 6.90 of [18]). The STSR orthogonal 4-pol mode also yields the velocity v , spectrum width σ_v and the copolar correlation coefficient ρ_{hv} at lag 2 as shown in [18].

B. Coherent Versus Incoherent Cross-Polar Power: A Limitation in the Effectiveness of ESP

The unwanted cross-polar power radiated by the antenna can be split in two components: the incoherent cross-polar power, and the coherent cross-polar power [19].

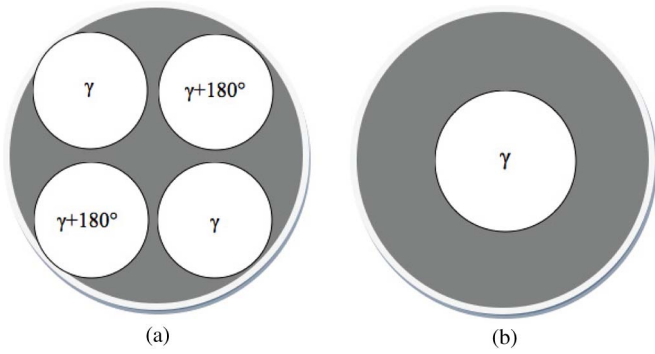


Fig. 2. Idealized antenna cross-polar patterns corresponding to incoherent cross-polar power (A), generally dominant in parabolic reflectors, and coherent cross-polar power (B), dominant in planar phased array antennas.

ESP only corrects for the **coherent** component of cross-polar power, and its effectiveness is uniquely established by the values (in drizzle/light rain) of the cross-polar correlation coefficient ρ_{xh} as will be later shown in Fig. 3 of Section II. Therefore, ESP always improves the performance of the antenna, but the extent of the improvement is driven by the coherent versus incoherent nature of the antenna cross-polar power.

Using the same symbols defined in [1] and indicating with F_h and F_x the one-way electric field complex copolar and cross-polar antenna patterns, respectively, we write the antenna first and second order pattern weighting functions

$$W_1 \equiv \frac{\int_{\Omega} F_h^3 F_x}{\int_{\Omega} F_h^4} \quad (1)$$

$$W_2 \equiv \frac{\int_{\Omega} F_h^2 F_x^2}{\int_{\Omega} F_h^4}. \quad (2)$$

Incoherent cross-polar power, coherent cross-polar power and total cross-polar power are respectively given by

$$P_{inc} = W_2 - W_1^2 \quad (3)$$

$$P_{co} = W_1^2 \quad (4)$$

$$P_{tot} = W_2. \quad (5)$$

For the case of completely coherent cross-polar power we have that $(W_1)^2 = W_2$, whereas for completely incoherent cross-polar power $W_1 = 0$ and $W_2 > 0$. With reference to [1, Eq. (66)], that we report here for convenience

$$\rho_{xh}^B \sim \sqrt{\frac{W_1^2}{W_2}} \quad (6)$$

it is useful to define the ratio χ of incoherent to coherent cross-polar power

$$\chi \equiv \frac{P_{inc}}{P_{co}} \quad (7)$$

to obtain a one-to-one relation between the measured cross-polar correlation coefficient and the incoherent-to-coherent cross-polar power ratio

$$\rho_{xh}^B = \frac{1}{\sqrt{1 + \chi^2}}. \quad (8)$$

When the contributions of coherent and incoherent cross-polar powers are equal, the measured cross-polar correlation coefficient is equal to $1/\sqrt{2} \sim 0.7$. Low cross-polar correlation coefficients (< 0.7) indicate that incoherent cross-polar power is dominant, whereas high cross-polar correlation coefficients (> 0.7) indicate that coherent cross-polar power is dominant. In general, minimum measurable LDR is the optimal metric to establish the polarimetric quality of the antenna, since it is one-to-one related to the total antenna cross-polar power W_2 , as shown by [1, Eq. (64)], whereas the cross-polar correlation coefficient does provide information about the coherent versus incoherent nature of cross-polar power as shown in (8).

Ideally, the incoherent cross-polar power appears as a quad of perfectly symmetric offset lobes of the cross-polar antenna pattern as shown in Fig. 2(a), and is produced by the natural geometry of the electric field lines on the radiating surface of the antenna [20]. The quad of offset cross-polar lobes is intrinsic to the parabolic reflectors as well as the microstrip patch antennas. When a cloud of spheres is illuminated (or, more generally, any target with reflection symmetry), such quad of offset lobes produces backscattered cross-polar power that is uncorrelated with the backscattered copolar power, and the cross-polar correlation coefficients (ρ_{xh} and ρ_{xv}) are equal to zero [1], [19]. The bias in polarimetric variables induced by incoherent cross-polar power cannot be removed by ESP. We will see in the ESP experiment in Section III that this is the case for the cc-off configuration, where the antenna in use is characterized by slightly high minimum measurable LDR (~ -26 dB) but low cross-polar correlation coefficient ($\rho_{xh} \sim 0.2-0.3$), and the dominance of incoherent cross-polar power compared to coherent cross-polar power is such that the improvement given by the application of ESP is small. In general, the effects of ESP are small in antennas with low ρ_{xh} (< 0.3) in drizzle/light rain as shown in Fig. 3. Examples are the recently modified CSU-CHILL [21] or the KOUN WSR-88D prototype at the National Severe Storms Laboratory in Norman, OK. For example, the effects of ESP on the KOUN radar are essentially undetectable: in that case, minimum measurable LDR (drizzle/light rain) is around -33 dB, and the corresponding ρ_{xh} is around 0.2 [7], indicating the presence of only a very small amount of incoherent cross-polar power (quad of offset lobes).

Coherent cross-polar power is generated by a number of sources. In the case of parabolic reflectors, it can be generated by imperfections in the reflector surface, feed-horn misalignment, finite isolation of the orthomode transducer or scattering from the feed support struts. In the case of a planar phased array scanning off the horizontal and vertical planes, it is generated by the misalignment of the radiated field lines with respect to the local horizontal [22]. The coherent cross-polar power significantly increases the cross-polar correlation coefficients (ρ_{xh} and ρ_{xv}), but the bias it introduces in the polarimetric

variables can be removed by ESP. We will see in Section III that this is the case of the cc-on configuration, where the bias in polarimetric variables induced by waveguide coupling can be accurately corrected by applying ESP.

II. THEORETICAL BACKGROUND

A. ESP: Eigenvalue Signal Processing

In this paragraph we reprise the concepts exposed in [1]. Weather radars at LDR mode measure the Coherency matrix at horizontal polarization transmit (\mathbf{J}_H), a matrix with 4 degrees of freedom. Note that this matrix is the upper left 2×2 minor of the backscatter covariance matrix in [23]

$$\mathbf{J}_H = \begin{bmatrix} \langle |s_{hh}|^2 \rangle & \langle s_{hh}^* s_{vh} \rangle \\ \langle s_{hh} s_{vh}^* \rangle & \langle |s_{vh}|^2 \rangle \end{bmatrix}. \quad (9)$$

From the Coherency matrix, radar variables are evaluated. From the two degrees of freedom on the diagonal, we can extract copolar reflectivity (Z_{HH}) cross-polar reflectivity (Z_{VH}) and the linear depolarization ratio (LDR_H)

$$Z_{HH} \propto \langle |s_{hh}|^2 \rangle \quad (10)$$

$$Z_{VH} \propto \langle |s_{vh}|^2 \rangle \quad (11)$$

$$LDR_H = \frac{\langle |s_{vh}|^2 \rangle}{\langle |s_{hh}|^2 \rangle}. \quad (12)$$

Reflectivity is proportional to the power backscattered at horizontal polarization, the linear depolarization ratio is representative of the target-induced coupling between copolar (horizontal) and cross-polar (vertical) channels. The two degrees of freedom on the off-diagonal term are captured by the cross-polar correlation coefficient (ρ_{xh}) and the cross-polar phase ψ_{xh} (propagation ϕ_{xh} plus back scatter δ_{xh})

$$\rho_{xh} = \frac{|\langle s_{hh}^* s_{vh} \rangle|}{\sqrt{\langle |s_{hh}|^2 \rangle \langle |s_{vh}|^2 \rangle}} \quad (13)$$

$$\psi_{xh} = \Phi_{xh} + \delta_{xh} = \arg[\langle s_{hh}^* s_{vh} \rangle]. \quad (14)$$

The cross-polar correlation coefficient ranges between 0 and 1, and is a normalized measure of the correlation between copolar and cross-polar signals. It is shown in [2] that cross-correlation departs from zero if and only if the target departs from reflection symmetry. Besides canted hydrometeors and ground clutter, aircrafts or other man-made objects can appear with positive, non-zero ρ_{xh} . The Coherency matrix \mathbf{J}_H can be diagonalized to yield

$$\mathbf{J}_H = \mathbf{U} \begin{bmatrix} \lambda_{H1} & 0 \\ 0 & \lambda_{H2} \end{bmatrix} \mathbf{U}^{-1} \quad (15)$$

where λ_{H1} and λ_{H2} are the largest and smallest eigenvalues, respectively, and \mathbf{U} indicates a unitary matrix. The trace (corresponding to the total backscattered power) and the degree of polarization at horizontal transmit (corresponding to the ratio

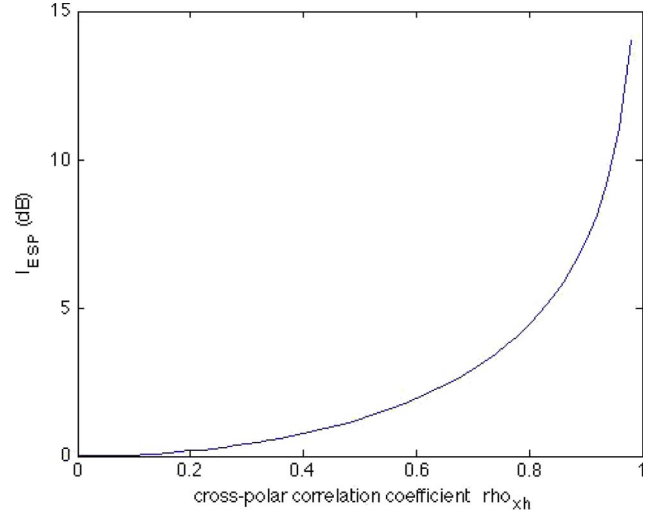


Fig. 3. Cross-polar correlation coefficient ρ_{xh} (on the abscissa) is one-to-one related to the ESP improvement factor I_{ESP} (on the ordinate), as shown in (26). For example, the minimum LDR of an antenna measuring $\rho_{xh} = 0.7$ in drizzle is lowered by 2.92 dB, minimum LDR of an antenna measuring $\rho_{xh} = 0.9$ in drizzle is lowered by 7.21 dB. The higher is the cross-polar correlation coefficient in drizzle/light rain, the larger is the improvement in minimum measurable LDR.

of completely polarized power to total power) are also derived from the eigenvalues

$$\text{Tr}\mathbf{J}_H = \lambda_{H1} + \lambda_{H2} \quad (16)$$

$$P_H = \frac{\lambda_{H1} - \lambda_{H2}}{\lambda_{H1} + \lambda_{H2}} = \sqrt{1 - \frac{4 \det \mathbf{J}_H}{[\text{Tr}\mathbf{J}_H]^2}}. \quad (17)$$

These variables can also be expressed in terms of the entries of the Coherency matrix \mathbf{J}_H as

$$\text{Tr}\mathbf{J}_H = \langle |s_{hh}|^2 \rangle + \langle |s_{vh}|^2 \rangle \quad (18)$$

$$P_H = \sqrt{1 - \frac{4 \left[\langle |s_{hh}|^2 \rangle \langle |s_{vh}|^2 \rangle - |\langle s_{hh} s_{vh}^* \rangle|^2 \right]}{[\langle |s_{hh}|^2 \rangle + \langle |s_{vh}|^2 \rangle]^2}}. \quad (19)$$

The degree of polarization at horizontal transmit is related to LDR_H and ρ_{xh} by a fundamental identity in radar polarimetry, obtainable by simple algebraic manipulation of (19) [24], [25]

$$(1 - P_H^2) = \frac{4LDR_H}{[1 + LDR_H]^2} (1 - \rho_{xh}^2). \quad (20)$$

The diagonalization of the Coherency matrix nulls the cross-polar correlation coefficient ρ_{xh} and the formula in (20) simplifies to

$$P_H = \frac{1 - LDR_H}{1 + LDR_H}. \quad (21)$$

Algebraic manipulation of (21) and (17) permits the definition of the first ESP variable: LDR_{H_ESP}

$$LDR_{H_ESP} \equiv \frac{\lambda_{H2}}{\lambda_{H1}}. \quad (22)$$

We note that LDR_{H_ESP} corresponds to LDR_H measured in the reference frame where ρ_{xh} is equal to 0. Therefore (21) should be rewritten as

$$p_H = \frac{1 - LDR_{H_ESP}}{1 + LDR_{H_ESP}}. \quad (23)$$

For an ideal antenna with no coherent cross-channel coupling (that is, an antenna that yields $\rho_{xh} = 0$ and $\rho_{xv} = 0$ when scatterers with reflection symmetry are illuminated), LDR_{H_ESP} is equal to LDR_H . In presence of coherent cross-channel coupling (that is, the antenna height spinor undergoes a small SU(2) rotation), LDR_H is positively biased, whereas LDR_{H_ESP} is not significantly biased. In general, the following inequality holds as shown in [1, Fig. 1(a)]

$$LDR_{H_ESP} \leq LDR_H. \quad (24)$$

It is possible to define the ESP improvement factor I_{ESP} as the ratio between LDR_H and LDR_{H_ESP}

$$I_{ESP} \equiv \frac{LDR_H}{LDR_{H_ESP}} \quad (25)$$

and by inserting (23) into (20), it is possible to prove that the ESP improvement factor I_{ESP} is one-to-one related to the cross-polar correlation coefficient ρ_{xh}

$$I_{ESP} = \frac{1}{1 - \rho_{xh}^2}. \quad (26)$$

A plot of (26) is reported in Fig. 3. The next step is the realization that the trace of the Coherency matrix \mathbf{J}_H is invariant for SU(2) transformations

$$\begin{aligned} \text{Tr}\mathbf{J}_H &= \langle |s_{hh}|^2 \rangle + \langle |s_{vh}|^2 \rangle = Z_{HH}[1 + LDR_H] \\ &= \lambda_{H1} + \lambda_{H2} = Z_{HH_ESP}[1 + LDR_{H_ESP}]. \end{aligned} \quad (27)$$

First, (27) links the bias in copolar reflectivity Z_{HH} to the bias in linear depolarization ratio LDR_H

$$\frac{Z_{HH_ESP}}{Z_{HH}} = \frac{1 + LDR_H}{1 + LDR_{H_ESP}}. \quad (28)$$

Secondly, (27) leads to the identification of the largest eigenvalue of the Coherency matrix (λ_{H1}) as the copolar (main) power received at LDR mode by an ‘‘aligned’’ antenna. This observation defines the second ESP variable

$$Z_{HH_ESP} \equiv \lambda_{H1}. \quad (29)$$

Also, it follows from (24) and (27) that the copolar power received by a perfectly aligned antenna is always larger than its biased counterpart. Equality only holds when the cross-polar power is purely incoherent

$$Z_{HH_ESP} \geq Z_{HH}. \quad (30)$$

The antenna-unbiased cross-polar reflectivity Z_{VH_ESP} is given by the smallest eigenvalue of the Coherency matrix and is always smaller than its biased counterpart Z_{VH}

$$Z_{VH_ESP} \equiv \lambda_{H2} \quad (31)$$

$$Z_{VH_ESP} \leq Z_{VH}. \quad (32)$$

The development above suggests a precise physical meaning for the eigenvalues of the Coherency matrix, that is, the largest and the smallest eigenvalues correspond to the copolar and cross-polar powers, respectively, as measured by an antenna whose antenna height spinor is perfectly aligned with the principal axes of the illuminated scatterers. The eigenvalues correspond to estimates of copolar and cross-polar powers that are unbiased by antenna coherent cross-polarization coupling; the unbiased depolarization ratio (LDR_{H_ESP}) is given by their ratio.

If the weather radar operates at ATSR or STSR orthogonal mode, the development above can also be applied to the Coherency matrix at vertical polarization transmit \mathbf{J}_V . Its largest and smallest eigenvalues can be indicated with λ_{V1} and λ_{V2} , respectively. The last eigenvalue-derived variable is the bias-corrected replacement for differential reflectivity Z_{DR} , which can be obtained as the ratio of the largest eigenvalues of the Coherency matrices at horizontal and vertical transmit

$$Z_{DR_ESP} \equiv \frac{Z_{HH_ESP}}{Z_{VV_ESP}} \equiv \frac{\lambda_{H1}}{\lambda_{V1}}. \quad (33)$$

Also, since antenna reciprocity implies that

$$\langle |s_{hv}|^2 \rangle = \langle |s_{vh}|^2 \rangle \quad (34)$$

we also have that the smallest eigenvalues of the Coherency matrices at H and V are equal

$$\lambda_{H2} = \lambda_{V2}. \quad (35)$$

The theory exposed in this section permits removal of the bias induced by antenna coherent cross-polarization coupling in power-like weather radar variables, specifically reflectivity Z , Linear Depolarization Ratio LDR and Differential Reflectivity Z_{DR} . It may have been noted that ESP does not provide replacements for variables derived from the 1,3 term of the covariance matrix, specifically the copolar correlation coefficient ρ_{hv} and the specific differential phase (KDP). This had to be expected, since ESP diagonalizes the 2×2 Coherency matrices \mathbf{J}_H and \mathbf{J}_V , but does not involve the 1,3 term of the Covariance matrix. However, the copolar correlation coefficient ρ_{hv} and the specific differential phase KDP, retrieved in the ATSR mode and STSR orthogonal 4-pol mode, are not significantly affected by antenna cross-channel coupling [16]. At STSR orthogonal mode, ESP is applicable for the retrieval of unbiased estimates of Z , Z_{DR} and LDR , and at the same time it does not pose any constraint on the waveforms in use. In the case of the STSR hybrid mode, ESP is not applicable, because the receive polarization basis is not orthogonal to the transmit polarization basis. Table II summarizes the radar meteorological variables and their eigenvalue-derived counterparts (far-right column).

TABLE II
ESP VARIABLES

<i>Name</i>	<i>Standard</i>	<i>ESP variables</i>
Reflectivity at horizontal transmit	Z_{HH}	Z_{HH_ESP}
Reflectivity at vertical transmit	Z_{VV}	Z_{VV_ESP}
Linear Depolariz. Ratio at horizontal tx	LDR_H	LDR_{H_ESP}
Linear Depolariz. Ratio at vertical tx	LDR_V	LDR_{V_ESP}
Differential Reflectivity	Z_{DR}	Z_{DR_ESP}
Copolar correlation coefficient	ρ_{hv}	-
Specific Differential phase	KDP	-

Even though not commonly used in radar meteorology, the degree of polarization and the trace of the coherency matrix (not listed in Table II) are also eigenvalue-derived variables, and automatically enjoy the property of being robust against antenna coherent cross-channel coupling.

B. Algebraic Evaluation of the Eigenvalues

Analytical expressions for the two eigenvalues of the Coherency matrix can be obtained as follows:

$$\det \begin{bmatrix} \langle |s_{hh}|^2 \rangle - \lambda_H & \langle s_{hh}s_{vh}^* \rangle \\ \langle s_{vh}s_{hh}^* \rangle & \langle |s_{vh}|^2 \rangle - \lambda_H \end{bmatrix} = 0 \quad (36)$$

$$\lambda_{H1,H2} = \frac{1}{2} \left[\langle |s_{hh}|^2 \rangle + \langle |s_{vh}|^2 \rangle \pm \sqrt{[\langle |s_{hh}|^2 \rangle - \langle |s_{vh}|^2 \rangle]^2 + 4 |\langle s_{hh}s_{vh}^* \rangle|^2} \right]. \quad (37)$$

The extreme cases of Eigenvalue Signal Processing are obtained for $\rho_{xh} = 0$ and $\rho_{xh} = 1$. For $\rho_{xh} = 0$, that is, for scatterers with reflection symmetry, the eigenvalues reduce to

$$\lambda_{H1} = \langle |s_{hh}|^2 \rangle \quad (38)$$

$$\lambda_{H2} = \langle |s_{vh}|^2 \rangle. \quad (39)$$

For $\rho_{xh} = 1$, that is, for some categories of canted scatterers (for example, a cloud of tilted dipoles all tilted at the same angle), the eigenvalues reduce to

$$\lambda_{H1} = \langle |s_{hh}|^2 \rangle + \langle |s_{vh}|^2 \rangle \quad (40)$$

$$\lambda_{H2} = 0. \quad (41)$$

This is consistent with the concept that the largest and smallest eigenvalues are the copolar and cross-polar powers as measured in the aligned reference frame, that is, in the reference frame where the cross-polar correlation coefficient ρ_{xh} is equal to 0. For scatterers with ρ_{xh} equal to 1, LDR in the aligned reference frame is 0 (linear units) and the copolar power in the aligned reference frame is equal to the copolar plus cross-polar power measured in the tilted reference frame, as indicated in (40).

The robustness of eigenvalue-derived variables with respect to antenna coherent cross-channel coupling can be tested with

a simple numerical simulation using [1, Eq. (56)]. For fully coherent coupling with $W_1 = -12.5$ dB and $W_2 = -25$ dB (note that for completely coherent coupling $W_1^2 = W_2$) for a population of raindrops with intrinsic LDR_H equal to -30 dB, intrinsic Z_{DR} equal to 0.5 dB, and intrinsic copolar correlation coefficient ρ_{hv} equal to 0.99, the biased LDR_H is equal to -18.92 dB but LDR_{H_ESP} is equal to -29.97 dB, much closer to the intrinsic LDR_H of -30 dB.

III. EIGENVALUE SIGNAL PROCESSING EXPERIMENT

Eigenvalue Signal Processing was tested at LDR mode for Z_{HH_ESP} , Z_{VH_ESP} , LDR_{H_ESP} , and DOP_H in an experiment conducted on November 10th 2012 at the Selex ES—Gematronik facilities in Neuss, Nordrhein-Westfalen, Germany [26] at around 16:20 local time, when ground temperature was $+11$ °C. The data were collected with a modified METEOR 600C dual-polarization Doppler weather radar, that can implement both the STSR hybrid mode and the LDR mode [27]. The parabolic reflector C-band antenna (wavelength 5.3 cm, beamwidth 1.0° —for more specifications, antenna is indicated as CLP10 in [28]), acquired a plan position indicator (PPI) at 1.5° elevation in a weather event consisting of light stratiform rain, with the melting band visible as a low LDR ring around the radar at about 50 km distance. Pulse Repetition Frequency (PRF) was 1300 Hz, range resolution was 0.15 km, antenna azimuth velocity was $4.8^\circ/s$, number of pulses per radial was 135 (collected over an angular interval of 0.5°). The radar was operated at LDR mode, in two different configurations indicated with cc-on (red curve in the plots) and cc-off (blue and green curves in the plots). The cc-on acquisition was taken between 16:18:20 and 16:19:40 CET (Central European Time), whereas the cc-off acquisition was taken between 16:19:40 and 16:21:00 CET. The two acquisitions are spaced in time by about 1.5 minutes, and it can reasonably be assumed that the illuminated scatterers are the same. By default, the radar is a hybrid design, that is, the transmitted pulse is split and fed with equal powers to the H and V waveguides, and reception occurs simultaneously in the H and V channels (STSR hybrid mode). In order to implement the standard LDR mode (indicated as cc-off in the following, that is, cross-coupling off), a remotely controlled mechanical waveguide switch redirects the full transmit power to the horizontal (H) polarization channel while the system still receives in both channels. To increase the antenna cross-polarization (indicated as cc-on in the following, that is, cross-coupling on) the system was modified as indicated in Fig. 4: the transmitter was directly connected to the H polarization transmit channel, a waveguide coupler (xpol coupler in Fig. 4) was inserted into the transmit channel and the extracted pulse was then injected into the vertical (V) polarization channel via the waveguide switch. This allows a quick on- and off-switching of the transmit cross-polarization. The difference in attenuation between the H and V antenna waveguide runs was $H/V = 0.75$ dB. The coupling loss of the xpol signal was 22.4 dB. The described set-up simulates coherent (coaxial) cross-polar power on transmission only, since on reception the antenna is still acceptably isolated,

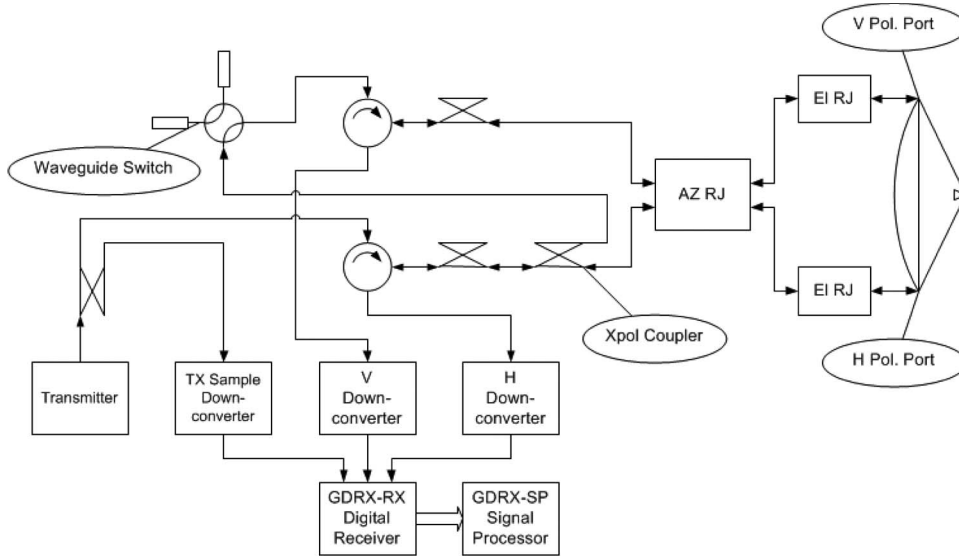


Fig. 4. Radar system block diagram for the cross-coupling on (cc-on) configuration. A 20 dB waveguide coupler (Xpol Coupler) extracts power from the H Tx waveguide and feeds it to the V Tx waveguide via the Waveguide switch.

and can be modeled with the following matrix multiplication (symbols are as in [1])

$$\mathbf{S}' = \mathbf{S}\mathbf{F} = \begin{bmatrix} s_{hh} & s_{hv} \\ s_{vh} & s_{vv} \end{bmatrix} \begin{bmatrix} F_{hh} & 0 \\ F_{vh} & F_{vv} \end{bmatrix} \begin{bmatrix} 1 \\ 0 \end{bmatrix}. \quad (42)$$

Depending on the exact hardware source of cross-polar power, the mathematical models may differ. The proposed experiment validates the robustness of ESP with respect to coaxial cross-polarization on transmit in radars with parabolic reflector antennas. The effects of antenna cross-coupling on transmit are the most relevant, since $SU(2)$ transformations of the Coherency matrix do exactly correspond to a change of the receive polarization basis, and therefore the invariance of eigenvalue-derived variables with respect to coherent cross-channel coupling on receive is mathematically exact. In the acquired PPIs (Fig. 5) considerable blockage occurs in the western sector, and interference appears as radial lines and arcs throughout the rest of the PPI disc. Radials for the analysis were chosen at azimuth angle of 352° , where the microwave ray only goes through light rain (from 10 to 40 km) and the melting band (from 45 to 60 km), but avoids more complex scattering situations like ground clutter (visible at around 25 km from the radar in the NE sector) and electromagnetic interference.

A. Experimental Verification of ESP Inequalities and ESP Improvement Factor

We start by analyzing the effects of ESP on the cc-off hardware configuration. The values of LDR_H and ρ_{xh} in drizzle/light rain provide a comprehensive characterization of the coherent and incoherent cross-polar power radiated by the antenna: minimum LDR_H is proportional to the total cross-polar power W_2 , whereas the cross-polar correlation coefficient ρ_{xh} is one-to-one related to the ratio of incoherent-to-coherent cross-polar power χ as shown in (8). In the cc-off configuration,

in light rain, the antenna yields slightly high values of LDR (~ -26 dB) and low values of ρ_{xh} [$\sim 0.2-0.3$, blue curve in Fig. 8(c)], indicating that incoherent cross-polar power is significantly dominant, and that the ESP improvement factor is minimal (incoherent cross-polar power present in the cc-off configuration cannot be removed by ESP). We apply ESP to the cc-off configuration to find that, in accordance with (26), eigenvalue-derived variables (ESP-on) differ only slightly from their standard (ESP-off) counterparts (Fig. 6). In Fig. 6, blue curves refer to the cc-off/ESP-off configuration, whereas green curves refer to the cc-off/ESP-on configuration. For the cc-off configuration, the difference between Z_{VH} and Z_{VH_ESP} and between LDR_H and LDR_{H_ESP} is visible [Fig. 6(b) and (c)], whereas the difference between Z_{HH} and Z_{HH_ESP} is not noticeable [Fig. 6(a)]. In Table III, mean and standard deviation of 101 data points between 15 and 30 km (light rain) are reported and do confirm the inequalities in (24) and (32). To ascertain the validity of the inequality in (30), we resorted to consider both cc-off and cc-on configurations, and we reported the differences between Z_{HH_ESP} and Z_{HH} in Fig. 7. We note how $Z_{HH_ESP} > Z_{HH}$ in the cc-on configuration [Fig. 7(b)], and how the difference between ESP and traditional variables grows larger for increasing levels of coherent cross-channel coupling. With reference to Fig. 7(b), we averaged 101 data points between 15 and 30 km from the radar (light rain), where the bias induced in copolar reflectivity Z_{HH} (specifically $Z_{HH_ESP} - Z_{HH}$ for the cc-on configuration) is 0.02241 dB. The corresponding difference between LDR_H and LDR_{H_ESP} [Fig. 8(d) and (e)] for the cc-on configuration for the same data points between 15 and 30 km is 4.82 dB, that, injected in (28), yields a predicted bias in copolar reflectivity of 0.02238 dB, in perfect agreement with the bias in copolar reflectivity Z_{HH} of 0.02241 experimentally observed in Fig. 7(b). We conclude that

- ESP inequalities in (24), (30), and (32) are experimentally verified.

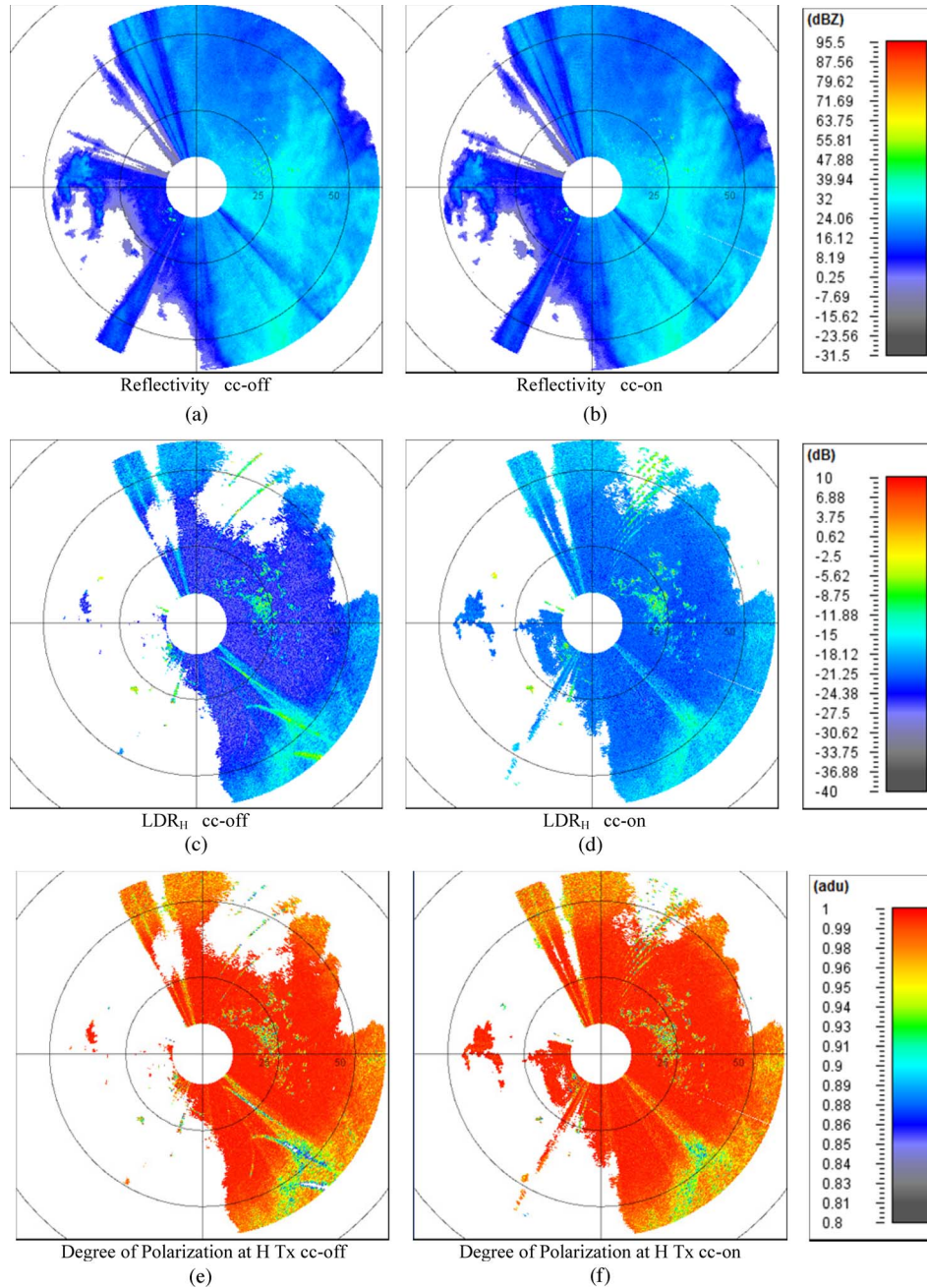


Fig. 5. Panels from A to F are PPIs at 1.5° elevation of polarimetric variables at LDR mode. The black circles indicate ranges of 25, 50, and 75 km, respectively. The PPIs on the left (Panels A, C, and E) correspond to data acquired in the cross-coupling off (cc-off) configuration; the PPIs on the right (Panels B, D, and F) correspond to data acquired in the cross-coupling on (cc-on) configuration. Rain is present between 10 and 50 km from the radar, the melting band appears as a low LDR_H/DOP_H ring beyond 50 km. Beam blockage is present in the western quadrants, clutter is present mainly in the first quadrant at about 25 km range. Interference appears as low LDR_H/DOP_H lines/arcs and changes characteristics between the two acquisitions (spaced in time 1.5 minutes). Copolar reflectivity is not significantly affected by coupling. LDR_H is affected by coupling, and good isolation (panel C) enhances the contrast between rain and the melting band with respect to poor isolation (panel D). LDR_{H_ESP} (not reported for compactness) is identical to LDR_H cc-off (panel C) and does recover the unbiased LDR_H field as shown in Fig. 8(e). Finally, DOP_H is invariant with respect to coherent cross-channel coupling, as can be qualitatively assessed by panels E and F, and further analyzed in Fig. 8(f). For the quantitative analysis, we select a radial at 352° azimuth, where only rain and wet aggregates (melting band) are present. (a) Reflectivity cc-off; (b) reflectivity cc-on; (c) LDR_H cc-off; (d) LDR_H cc-on; (e) degree of polarization at H Tx cc-off; (f) degree of polarization at H Tx cc-on.

- Equation (28) provides an accurate relation between the bias in Z_{HH} and the bias in LDR_H .
- Equation (26) provides an accurate relation between the measured cross-polar correlation coefficient and the ESP improvement factor. In particular, for antennas where incoherent cross-polar power is largely dominant (ρ_{xh} in

drizzle/light rain is less than 0.4), the improvement given by ESP is small, as shown in Fig. 6.

We note how application of ESP in antennas dominated by incoherent cross-polar power may still be beneficial to remove propagation effects due to coherent forward scattering

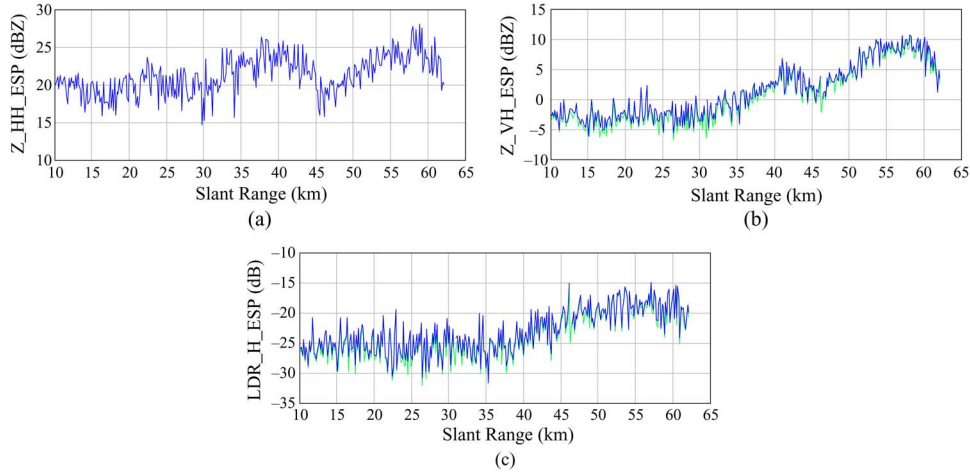


Fig. 6. Comparison of ESP-on and ESP-off versions of Z_{HH} , Z_{VH} , and LDR_H for the cc-off configuration. When incoherent cross-polar power is dominant (ρ_{xh} is about 0.3 for the cc-off configuration) ESP produces only small changes in Z_{VH} and LDR_H , in agreement with the theory of Section II. (a) Copolar reflectivity ESP-off (Z_{HH} , blue curve) and copolar reflectivity ESP-on (Z_{HH_ESP} , green curve) for the cc-off configuration. With ρ_{xh} equal to about 0.3 [Fig. 8(c), blue curve], the application of ESP does not noticeably affect copolar reflectivity, and the blue and green curves are perfectly superimposed. (b) Cross-polar reflectivity ESP-off (Z_{VH} , blue curve) and cross-polar reflectivity ESP-on (Z_{VH_ESP} , green curve) for the cc-off configuration. The application of ESP lowers cross-polar reflectivity as predicted in (32). (c) Linear Depolarization Ratio ESP-off (LDR_H , blue curve) and Linear Depolarization Ratio ESP-on (LDR_{H_ESP} , green curve) for the cc-off configuration. The application of ESP lowers LDR_H as predicted in (24).

TABLE III
AVERAGED DATA POINTS BETWEEN 15 AND 30 km
(LIGHT RAIN) FOR CC-OFF

	<i>Mean</i>	<i>Standard Deviation</i>
Z_{HH}	19.62 dBZ	1.86 dBZ
Z_{HH_ESP}	19.62 dBZ	1.86 dBZ
Z_{VH}	-2.61 dBZ	1.58 dBZ
Z_{VH_ESP}	-3.31 dBZ	1.66 dBZ
LDR_H	-25.35 dB	2.48 dB
LDR_{H_ESP}	-26.05 dB	2.56 dB

from canted hydrometeors, as shown in [7] for the Degree of Polarization at horizontal transmit.

B. Removing the Bias Induced by Coherent Cross-Channel Coupling: Comparison Between cc-Off and cc-On Configurations

We now compare results from the cc-off/ESP-off configuration (blue curves) with the cc-on/ESP-on and cc-on/ESP-off configurations (red curves). In the cc-on configuration cross-polar isolation is significantly lowered (LDR in light rain is about -21 dB), but the additional cross-polar power is coherent, as indicated by the higher cross-polar correlation coefficient [Fig. 8(c), $\rho_{xh} \sim 0.8$] and the bias in polarimetric variables is effectively removed by ESP (Fig. 8). Fig. 8(c) shows that, in drizzle/light rain between 15 and 30 km, for the cc-off configuration, the antenna yields values of ρ_{xh} around 0.3, whereas for the cc-on configuration the antenna yields values around 0.8. In agreement with the theory, coherent cross-channel coupling (induced by the cc-on configuration) increases the measured cross-polar correlation coefficient. In Fig. 8(a), standard (ESP-off) cross-polar reflectivity (Z_{VH}) from the cc-on (red curve) and cc-off (blue curve) configurations are compared. We can

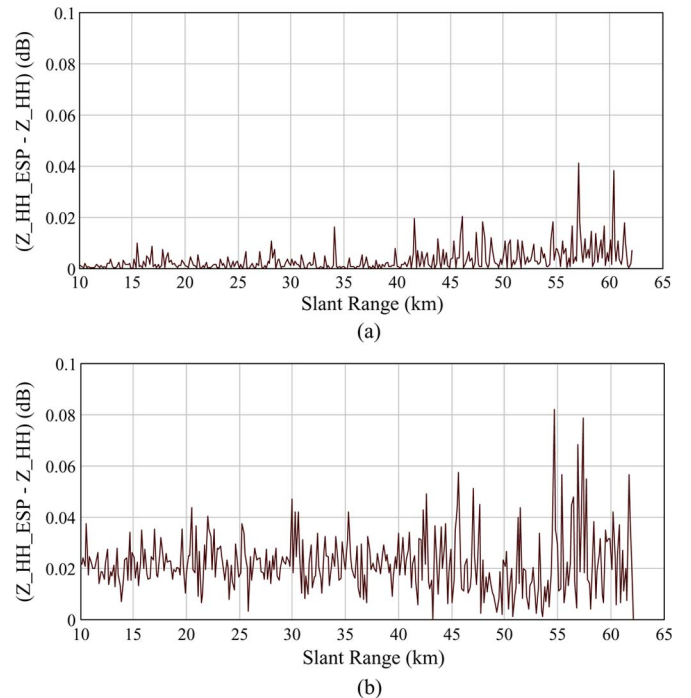


Fig. 7. Difference between Z_{HH_ESP} and Z_{HH} for the cc-off (A) and cc-on (B) configurations. The difference of 0.02241 dBZ in copolar reflectivity ($Z_{HH_ESP} - Z_{HH}$) measured between 15 and 30 km in B is in excellent agreement with the difference of 4.82 dB between LDR_H and LDR_{H_ESP} in Fig. 8(d), as predicted by (28). For increasing levels of coherent cross-channel coupling, the difference between ESP and standard variables becomes larger. (a) Difference between Z_{HH_ESP} and Z_{HH} is negligible for the cc-off configuration ($\rho_{xh} \sim 0.3$). (b) Difference between Z_{HH_ESP} and Z_{HH} is small but noticeable for the cc-on configuration ($\rho_{xh} \sim 0.8$).

observe that cross-channel coupling (induced by the cc-on configuration) increases cross-polar reflectivity. In Fig. 8(b), Eigenvalue Signal Processing is applied to data collected in the cc-on configuration (red curve), and compared to standard (ESP-off) cross-polar reflectivity from the cc-off configuration [blue curve in Fig. 6(b) is the same as blue curve in Fig. 8(a)]

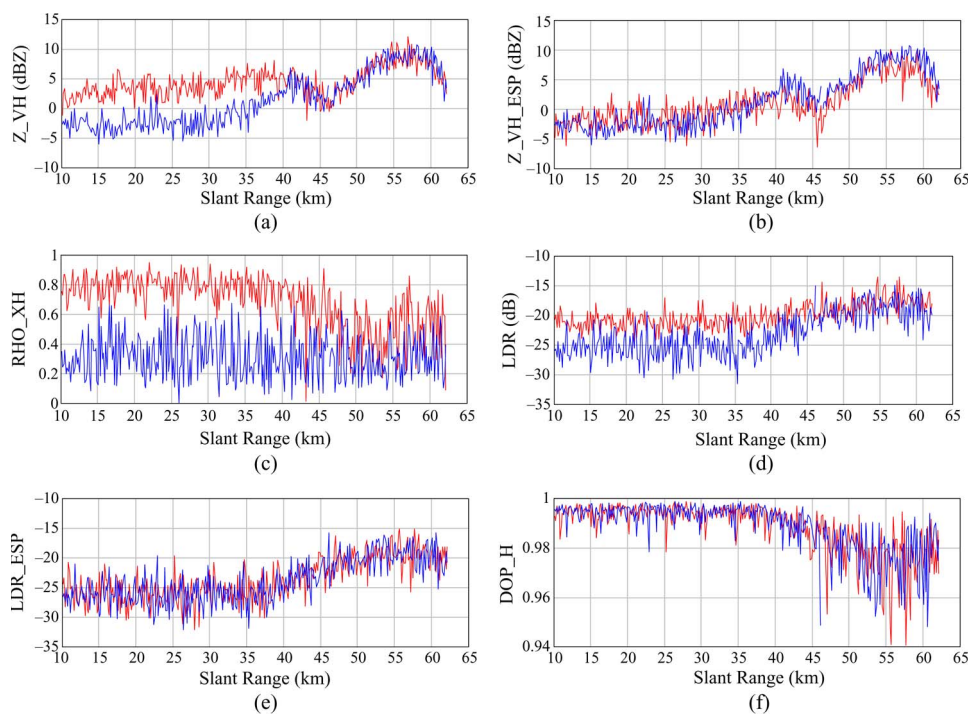


Fig. 8. Radial plots for 352° azimuth (between 352° and 352.5°). The radial goes through rain (10–40 km) and then through the melting band (> 40 km). The word “standard” refers to standard signal processing (ESP-off), the term “ESP-corrected” refers to the eigenvalue-derived variables (ESP-on). In the panels from A to F, standard polarimetric variables from the cc-off configuration (blue curves) are compared with standard and ESP-corrected polarimetric variables from the cc-on configuration (red curves). (a) Standard cross-polar reflectivity Z_{VH} (ESP-off) for the cc-off (blue) and cc-on (red) configurations. Cross-channel coupling (cc-on, red curve) increases cross-polar reflectivity with respect to the cc-off configuration. This phenomenon is well visible in rain, between 10 and 40 km and less visible in the melting band (50–60 km). (b) Standard cross-polar reflectivity Z_{VH} (dBZ) for the cc-off configuration as in A (blue curve), superimposed with ESP-corrected cross-polar reflectivity (smallest eigenvalue) obtained from the cc-on configuration: Z_{VH_ESP} (red curve). By comparing A and B we can observe that Eigenvalue Signal Processing lowers cross-polar in rain (10–40 km) and in the melting band (50–60 km) to levels below the cc-off configuration, as predicted by the theory. Note how ESP increases the overall reflectivity dynamic range of Z_{VH} . (c) Cross-polar correlation coefficient ρ_{xh} . The cross-polar correlation coefficient provides a measurement of antenna coherent cross-channel coupling. The red curve refers to the cc-on configuration (high ρ_{xh}), the blue curve refers to the cc-off configuration (low ρ_{xh}). (d) Linear depolarization ratio (dB). LDR_H is affected by antenna coupling as it is clearly illustrated by the red curve (standard LDR_H corresponding to cc-on) and blue curve, (standard LDR_H corresponding to cc-off). The difference is blurred after 45 km, where more depolarizing scatterers (melting band) are present, and the effects of imperfect isolation become less visible. Lack of polarimetric purity decreases the polarimetric contrast and makes discrimination more difficult. (e) Linear depolarization ratio (dB). Blue curve is standard LDR_H for the cc-off configuration (same as blue curve in D), red curve is ESP-corrected LDR (LDR_{H_ESP}) from the cc-on configuration. Eigenvalue Signal Processing recovers the unbiased LDR_H (red curve superimposes with the blue curve) and restores the dynamic range corresponding to the cc-off configuration. In general, $LDR_{H_ESP} \leq LDR_H$. (f) Degree of polarization at horizontal transmit (DOP_H). The degree of polarization at horizontal transmit can be expressed in terms of the eigenvalues of the Coherency matrix, and is therefore invariant with respect to coherent cross-channel coupling, as clearly indicated by the superimposed red and blue curves corresponding to the cc-on and cc-off configurations, respectively.

and (b)]. We can observe that ESP lowers cross-polar reflectivity to values lower than those corresponding to the ESP-off/cc-off configuration. Specifically, ESP-corrected cross-polar reflectivity (Z_{VH_ESP} , that is, the smallest eigenvalue) is lower than standard (ESP-off) cross-polar reflectivity from the cc-off configuration (Z_{VH}) because, even in the cc-off configuration, some residual coherent cross-channel coupling is present ($\rho_{xh} \sim 0.3$ in Fig. 8(c), blue curve).

Fig. 8(d) contains standard (ESP-off) LDR_H from the cc-on (red curve) and cc-off (blue curve) configurations. It can be observed that cross-channel coupling increases LDR_H by a significant amount. Such increase is more visible in weakly depolarizing scatterers like light rain, and less visible in the melting band. The dynamic range of LDR_H is reduced by increased cross-channel coupling, and therefore poor antenna isolation reduces the polarimetric contrast between different target types. Fig. 8(e) shows that application of ESP to data acquired in the cc-on configuration (LDR_{H_ESP}) retrieves values almost identical to the cc-off configuration. Note that

not only ESP lowers the minimum LDR, but also restores the dynamic range corresponding to the cc-off configuration.

We proceeded to a quantitative analysis of 101 data points between 15 and 30 km (light rain), for which the mean LDR_{H_ESP} (from cc-on) is -25.94 dB, whereas the mean LDR_H from the cc-off configuration is -25.35 dB (difference is 0.59 dB). This is in agreement with the theory, predicting $LDR_{H_ESP} \leq LDR_H$. The standard deviation for LDR_H cc-off was 2.48 dB and for LDR_{H_ESP} was 2.4 dB. This latter measurement suggests that ESP variables (that indirectly incorporate the noisy cross-polar correlation coefficient) are not affected more by noise than their standard counterparts. The mean LDR_H for the cc-on configuration (ESP-off) was -21.12 dB with a standard deviation of 1.42 dB. For this particular antenna, in light rain between 15 and 30 km, application of ESP expands the dynamic range of the depolarization ratio by 4.82 dB, in perfect agreement with the bias of 0.022 dBZ in copolar reflectivity observed in Fig. 7(b). Fig. 8(f) gives yet another experimental proof of the concepts exposed in [1] and

shows that the Degree of Polarization at horizontal transmit DOP_H is robust with respect to antenna coherent cross-channel coupling.

ESP theory assumes target reflection symmetry and, under such assumption, LDR_{H_ESP} and DOP_H are one-to-one related, and therefore these two variables contain the same microphysical information. The ESP experiment leads to the conclusion that eigenvalue-derived variables [$Z_{HH_ESP} \equiv \lambda_{H1}$, $Z_{VH_ESP} \equiv \lambda_{H2}$, $LDR_{H_ESP} \equiv \lambda_{H2}/\lambda_{H1}$, $DOP_H = (\lambda_{H1} - \lambda_{H2})/(\lambda_{H1} + \lambda_{H2})$] are robust with respect to antenna coherent cross-channel coupling, whereas standard variables ($Z_{HH} \equiv \langle |s_{hh}|^2 \rangle$, $Z_{VH} \equiv \langle |s_{vh}|^2 \rangle$, $LDR_H \equiv \langle |s_{vh}|^2 \rangle / \langle |s_{hh}|^2 \rangle$), simply derived from the entries of the Coherency matrix, are not. Eigenvalue Signal Processing provides an accurate mathematical framework for the quantitative analysis of the bias induced by antenna coherent and incoherent cross-channel coupling in polarimetric weather radar variables, and permits the retrieval of polarimetric variables (Z_{HH} and LDR_H) unbiased by coherent cross-channel coupling. Any bias induced by incoherent cross-channel coupling will still be present in the ESP estimates.

IV. CONCLUSION

Eigenvalue Signal Processing is a novel polarimetric signal processing procedure that permits the removal of the bias induced by antenna coherent cross-polar power in weather radar variables, specifically in reflectivity Z , differential reflectivity Z_{DR} and linear depolarization ratio LDR . It is applicable in polarimetric weather radars operating at LDR, ATSR and STSR orthogonal modes. It is not applicable at STSR hybrid mode, since it requires orthogonal polarization bases. The strength of the approach is that bias correction is effected automatically by means of the diagonalization of the Coherency matrices at horizontal and vertical polarizations, and knowledge of the actual amount of cross-polar power radiated by the antenna is not necessary.

ESP is effective for the removal of the biases induced by coherent cross-polar power (coaxially radiated cross-polar power) but cannot remove the biases due to incoherent cross-polar power (radiated as a quad of offset lobes). Consequently, the effectiveness of the ESP technique is dependent on the spatial structure of cross-polar power and varies from antenna to antenna. For the case reported in the present paper of artificially induced waveguide coupling in a Gematronik METEOR 600C, the improvement in LDR is of about 5 dB.

In this paper, the theory of Eigenvalue Signal Processing was experimentally tested at LDR mode for copolar reflectivity Z_{HH} , cross-polar reflectivity Z_{VH} , Linear Depolarization Ratio LDR_H and Degree of Polarization DOP_H . In particular, it is demonstrated that ESP can recover the unbiased LDR , named LDR_{ESP} , with the dynamic range corresponding to an antenna solely affected by incoherent cross-polar power. The robustness with respect to antenna coherent cross-channel coupling of the degree of polarization at horizontal transmit DOP_H is experimentally proven, as theoretically analyzed in [1]. Under the assumption of reflection symmetry, LDR_{ESP} and DOP_H are one-to-one related, and therefore contain the same

microphysical information. Use of eigenvalue-derived variables is recommended to enhance the polarimetric performance of radars at LDR, ATSR and STSR orthogonal modes in presence of parabolic reflector antennas with imperfect polarimetric isolation. Ongoing work involves experimental testing with planar phased-array antennas and will also consider the fully polarimetric aspects of ESP, specifically the retrieval of antenna unbiased estimates of differential reflectivity Z_{DR} .

REFERENCES

- [1] M. Galletti, D. S. Zrnica, V. M. Melnikov, and R. J. Doviak, "Degree of polarization at horizontal transmit: Theory and applications for weather radar," *IEEE Trans. Geosci. Remote Sens.*, vol. 50, no. 4, pp. 1291–1301, Apr. 2012.
- [2] S. V. Nghiem, S. H. Yueh, R. Kwok, and F. K. Li, "Symmetry properties in polarimetric remote sensing," *Radio Sci.*, vol. 27, no. 5, pp. 693–711, Sep./Oct. 1992.
- [3] A. Zahrai and D. Zrnica, "Implementation of polarimetric capability for the WSR-88D (NEXRAD) radar," in *Proc. IEEE NAECON*, Jul. 14–18, 1997, vol. 1, pp. 346–352.
- [4] D. Bebbington and L. Carrea, "Geometric polarimetry—Part I: Spinors and wave states," *IEEE Trans. Geosci. Remote Sens.*, vol. 52, no. 7, pp. 3908–3923, Jul. 2014.
- [5] C. D. Graves, "Radar polarization power scattering matrix," *Proc. IRE*, vol. 44, no. 2, pp. 248–252, Feb. 1956.
- [6] J. M. Kwiatkowski, A. B. Kostinski, and A. R. Jameson, "The use of optimal polarizations for studying the microphysics of precipitation: Nonattenuating wavelengths," *J. Atmos. Ocean. Technol.*, vol. 12, no. 1, pp. 96–114, Feb. 1995.
- [7] M. Galletti, D. S. Zrnica, V. M. Melnikov, and R. J. Doviak, "Degree of polarization: Theory and applications for weather radar at LDR mode," in *Proc. IEEE Radar Conf.*, May 23–27, 2011, pp. 039–044.
- [8] S. R. Cloude and E. Pottier, "A review of target decomposition theorems in radar polarimetry," *IEEE Trans. Geosci. Remote Sens.*, vol. 34, no. 2, pp. 498–518, Mar. 1996.
- [9] J.-S. Lee and E. Pottier, *Polarimetric Radar Imaging: From Basics to Applications*. Boca Raton, FL, USA: CRC Press, 2009.
- [10] S. R. Cloude, "Lie Groups in electromagnetic wave propagation and scattering," in *Electromagnetic Symmetry*, C. E. Baum and H. N. Kritikos, Eds. New York, NY, USA: Taylor & Francis, 1995, ch. 2.
- [11] M. Galletti, D. H. O. Bebbington, M. Chandra, and T. Boerner, "Measurement and characterization of entropy and degree of polarization of weather radar targets," *IEEE Trans. Geosci. Remote Sens.*, vol. 46, no. 10, pp. 3196–3207, Oct. 2008.
- [12] M. Galletti, M. Chandra, T. Borner, and D. H. O. Bebbington, "Degree of polarization for weather radars," *Proc. IGARSS*, pp. 4187–4190, Jul. 23–28, 2007.
- [13] D. Giuli, M. Fossi, and L. Facheris, "Radar target scattering matrix measurement through orthogonal signals," *Proc. Inst. Elect. Eng.-F Radar Signal Process.*, vol. 140, no. 4, pp. 233–242, Aug. 1993.
- [14] D. Giuli, L. Facheris, M. Fossi, and A. Rossetini, "Simultaneous scattering matrix measurement through signal coding," in *Proc. IEEE Int. Radar Conf.*, May 7–10, 1990, pp. 258–262.
- [15] V. Chandrasekar and N. Bharadwaj, "Orthogonal channel coding for simultaneous co- and cross-polarization measurements," *J. Atmos. Ocean. Technol.*, vol. 26, no. 1, pp. 45–56, Jan. 2009.
- [16] Y. Wang and V. Chandrasekar, "Polarization isolation requirements for linear dual-polarization weather radar in simultaneous transmission mode of operation," *IEEE Trans. Geosci. Remote Sens.*, vol. 44, no. 8, pp. 2019–2028, Aug. 2006.
- [17] E. A. Mueller, "Calculation procedures for differential propagation phase shift," in *Proc. 22nd Conf. Radar Meteorol.*, 1984, pp. 397–399.
- [18] V. N. Bringi and V. Chandrasekar, *Polarimetric Doppler Weather Radar. Principles and Applications*. Cambridge, U.K.: Cambridge Univ. Press, 2001.
- [19] D. S. Zrnica, R. J. Doviak, G. Zhang, and A. Ryzhkov, "Bias in differential reflectivity due to cross-coupling through radiation patterns of polarimetric weather radars," *J. Atmos. Ocean. Technol.*, vol. 27, no. 10, pp. 1624–1637, Oct. 2010.
- [20] A. Z. Fradin, *Microwave Antennas*. London, U.K.: Pergamon, 1961.
- [21] V. N. Bringi et al., "Design and performance characteristics of the new 8.5-m dual-offset gregorian antenna for the CSU-CHILL radar," *J. Atmos. Ocean. Technol.*, vol. 28, no. 7, pp. 907–920, Jul. 2011.

- [22] G. Zhang *et al.*, "Phased array radar polarimetry for weather sensing: A theoretical formulation for bias correction," *IEEE Trans. Geosci. Remote Sens.*, vol. 47, no. 11, pp. 3679–3689, Nov. 2009.
- [23] R. J. Doviak and D. S. Zrnica, *Doppler Radar and Weather Observations*, 2nd ed. San Diego, CA, USA: Academic Press, 1993.
- [24] E. Wolf, "Coherence properties of partially polarized electromagnetic radiation," *Il Nuovo Cimento*, vol. 13, no. 6, pp. 1165–1181, Sep. 1959.
- [25] M. Born and E. Wolf, *Principles of Optics: Electromagnetic Theory of Propagation, Interference and Diffraction of Light*, 7th ed. Cambridge, U.K.: Cambridge Univ. Press, 1999.
- [26] [Online]. Available: <https://maps.google.com/maps?q=Selex+Systems+Integration+GmbH,+Raiffeisenstra%C3%9F+Neuss,+Germany&hl=en&ie=UTF8&ll=51.131554,6.735869&spn=0.001171,0.003575&sll=40.906488,-72.884172&sspn=0.180595,0.457649&oq=Selex+systems+inte&t=h&z=19>
- [27] [Online]. Available: <http://www.gematronik.com/products/radar-systems/meteor-600c-635c/>
- [28] [Online]. Available: http://www.gematronik.com/fileadmin/media/pdf/ProductDatasheet/METEOR_600C-635C_engl_1907154815.pdf
- [29] D. Moisseev, C. Unal, H. Russchemberg, and L. Ligthart, "A new method to separate ground clutter and atmospheric reflections in the case of similar Doppler velocities," *IEEE Trans. Geosci. Remote Sens.*, vol. 40, no. 2, pp. 239–246, Feb. 2002.
- [30] D. N. Moisseev, C. M. H. Unal, H. W. J. Russchenberg, and L. P. Ligthart, "Improved polarimetric calibration for atmospheric radars," *J. Atmos. Ocean. Technol.*, vol. 19, no. 12, pp. 1968–1977, Dec. 2002.
- [31] M. Galletti, "Fully polarimetric analysis of weather radar signatures," Ph.D. dissertation, TU Chemnitz, Chemnitz, Germany.
- [32] M. Galletti, D. H. O. Bebbington, M. Chandra, and T. Boerner, "Fully polarimetric analysis of weather radar signatures," in *Proc. IEEE Radar Conf.*, Rome, Italy, May 2008.
- [33] A. Ryzhkov *et al.*, "Polarimetric radar observations and interpretation of co-cross-polar correlation coefficients," *J. Atmos. Ocean. Technol.*, vol. 19, no. 3, pp. 340–354, Mar. 2002.
- [34] A. V. Ryzhkov, "Interpretation of polarimetric radar covariance matrix for meteorological scatterers: Theoretical analysis," *J. Atmos. Ocean. Technol.*, vol. 18, no. 3, pp. 315–328, Mar. 2001.
- [35] V. M. Melnikov, "One-lag estimators for cross-polarization measurements," *J. Ocean. Atmos. Technol.*, vol. 23, no. 7, pp. 915–926, Jul. 2006.
- [36] ESP Patent Application. [Online]. Available: http://worldwide.espacenet.com/publicationDetails/originalDocument?CC=WO&NR=2013192308A1&KC=A1&FT=D&ND=3&date=20131227&DB=EPODOC&locale=en_EP



Michele Galletti was born on November 13, 1978, in Bologna, Italy. He received the Ph.D. degree in electrical engineering from the Technische Universität Chemnitz, Chemnitz, Germany (funded by the European Commission through the AMPER project) and also with the Microwaves and Radar Institute of the German Aerospace Center (DLR-HR in Wessling, Germany).

In 2009, he was awarded a National Research Council postdoctoral position at the National Severe Storms Laboratory in Norman, OK, USA. During

this period, he worked on projects related to polarimetric phased array weather radars. Currently a member of the Radar Science Group at BNL, his research interests cover a wide span of weather and climate radar science topics at many frequencies (S, C, X, Ka, W, and beyond), with a focus on the theory and applications of radar polarimetry for atmospheric remote sensing.



Dusan S. Zrnica (F'90) was born on June 3, 1942, in Belgrade, Serbia. He graduated from the University of Belgrade, Belgrade, Serbia, with the Dipl.-Ing. degree in electrical engineering in 1965, and he obtained the M.Sc. (1966) and the Ph.D. (1969) degrees in electrical engineering from the University of Illinois, Urbana, IL, USA.

He is Leader of the Doppler Radar and Remote Sensing Research at the National Severe Storms Laboratory (NSSL) and Adjunct Professor of Meteorology and Electrical Engineering at the University of Oklahoma, Norman, OK, USA. Following employment as a research and teaching assistant with the Charged Particle Research Laboratory at the University of Illinois, he joined the Electrical Engineering Department of the California State University, Northridge, CA, USA. He became Associate Professor in 1974, and Professor in 1978. During the 1973–1974 academic year, he was a National Research Council Postdoctoral Fellow at the NSSL, and in 1975–1976 he was on sabbatical research leave from California State University at the same laboratory. His principal experience is in weather radar technology and radar meteorology including signal processing, polarimetric measurements and their interpretation, development of algorithms for NEXRAD, quantitative precipitation measurements, and systems design. He served five years as chief editor of the *Journal of Atmospheric and Oceanic Technology*. He has published extensively on weather radar signal processing, radar meteorology, and remote sensing. His most important and representative publication is the book *Doppler Radar and Weather Observations* (Academic Press, 1984, second edition 1993, paperback reprint by Dover 2006, coauthored with Dr. Richard Doviak).

Prof. Zrnica is a co-recipient of the IEEE 1988 Harry Diamond Memorial Award for contributions to and applications of weather radar science; he is sharing the 1993 IEEE Donald G. Fink Prize Award with Dr. P. Mahapatra, and is a recipient with R.V. Ryzhkov of the WMO 1996 Vaisala award. Four times he received the Best Research Paper Award within the NOAA's Ocean and Atmospheric Research office. He holds three U.S. patents in the area of weather radar technology. Since 1976 he has been a member of URSI Commissions C and F; he is a Fellow of the AMS. In 2004, he became a recipient of the Presidential Rank Award for exceptional long term accomplishments. He was inducted into the USA National Academy of Engineering in 2006 with citation: "For development of potent radar methods that have greatly enhanced operational weather detection and warning and advanced meteorological research." He was recognized by the AMS Remote Sensing Prize in 2008: "For pioneering and substantial contributions to improvements of meteorological radars for both research and operational applications." NOAA 2010 Technology Transfer Award was given to him for "developing a method that allows faster updates of dual-polarized radar data without losing function and provides significant cost savings."

Prof. Zrnica is a co-recipient of the IEEE 1988 Harry Diamond Memorial Award for contributions to and applications of weather radar science; he is sharing the 1993 IEEE Donald G. Fink Prize Award with Dr. P. Mahapatra, and is a recipient with R.V. Ryzhkov of the WMO 1996 Vaisala award. Four times he received the Best Research Paper Award within the NOAA's Ocean and Atmospheric Research office. He holds three U.S. patents in the area of weather radar technology. Since 1976 he has been a member of URSI Commissions C and F; he is a Fellow of the AMS. In 2004, he became a recipient of the Presidential Rank Award for exceptional long term accomplishments. He was inducted into the USA National Academy of Engineering in 2006 with citation: "For development of potent radar methods that have greatly enhanced operational weather detection and warning and advanced meteorological research." He was recognized by the AMS Remote Sensing Prize in 2008: "For pioneering and substantial contributions to improvements of meteorological radars for both research and operational applications." NOAA 2010 Technology Transfer Award was given to him for "developing a method that allows faster updates of dual-polarized radar data without losing function and provides significant cost savings."



Frank Gekat was born in Velbert, Germany, on December 14, 1957. He received the Dipl.-Ing. and Dr.-Ing. degrees in electrical engineering from Ruhr University Bochum, Bochum, Germany, in 1985 and 1992, respectively.

From 1981 to 1985, he was a student member of several research teams with the Institute of Electrooptics and Electrical Discharges, Ruhr-University Bochum, where he was involved in the development of HeSe metal vapor lasers, near-infrared HeNe lasers, heterodyne receivers, and RF excitation of rare-gas discharges. In 1985, he joined the German Aerospace Center (DLR), where he worked on high-power microwave excitation of excimer lasers. From 1992 to 1993, he was responsible for the project engineering of high-power microwave sources at Siemens Accelerator and Magnet Technology. In 1993, he joined Selex ES GmbH, Neuss, Germany, where he has been the Development Director since 1995.



Peter Goelz was born in Albstadt, Germany, in 1963. He received the Ph.D. degree (Dr. rer. nat.) in 1996 from Bielefeld University, Bielefeld, Germany, where he worked on UV laser spectroscopy.

From 1996 to 1998, he was with the AIP-Institute in Hagen (Germany), where he worked on optical measurement technologies. In 1998, he joined Selex ES GmbH, Neuss, Germany, where he is currently a Signal Processing Software Engineer. His current research interests at Selex ES GmbH include the development of operational software for commercial ground-based weather radars at S-, C-, and X-bands.